DNIPRO UNIVERSITY of TECHNOLOGY 1899

Mining of Mineral Deposits

Volume 15 (2021), Issue 3, 108-121

MMD JOURNAL / MINING.IN.UA

UDC 622.02+622.03

https://doi.org/10.33271/mining15.03.108

Geochemical characterization of the Sutlegen bauxite deposit, SW Antalya

Ozge Ozer Atakoglu[1*], Mustafa Gurhan Yalcin[1]

[1]*Akdeniz University, Antalya, 07058, Turkey*

**Corresponding author: e-mail oozer@akdeniz.edu.tr, tel. +2422274341*

Abstract

Purpose. The purpose is to determine geological and geochemical characteristics of the Sutlegen (Antalya, Turkey) bauxites, to identify the elements that played a major role in their formation.

Methods. X-ray diffraction (XRD) mineral phase analysis, X-ray fluorescence (XRF) elemental analysis, plasma-mass spectrometry (ICP-MS), the petrographic and mineralogical analyses, and multivariate statistical methods were used.

Findings. The major element content of the ore was determined as Al_2O_3 (60-35.2 wt%), SiO_2 (39.5-0.2 wt%), Fe_2O_3 (48.4-19.5 wt%), TiO_2 (36.9-16 wt%), and P_2O_5 (0.5-0.1 wt%). The Sutlegen region, which shows epirogenetic action with the uplift of the earth's crust, is generally rich in neritic carbonates. It was revealed that the bauxite ores have undergone moderate and strong laterization as a result of the deferruginization in the environment, and they were classified into four groups as lateritic, ferritic, kaolinitic, and bauxite. The increase in the aluminosilicate minerals, which were formed during the formation of bauxite in the environment was found to be directly proportional to the laterization processes. In this context, it was considered that the lateritic material that was firstly formed in the environment filled the cavities and pores of the karst-type limestones and sedimentary units in the region by superficial transfer phenomena. The bivariate diagrams of Log Cr vs. Log Ni revealed that the bauxite that formed in the region had an ultrabasic source.

Originality. In literature, no scientific studies have been found on bauxite mineralization in the Sutlegen deposits that have been operated for a long period.

Practical implications. In this context, the geochemical characteristics of bauxites revealed that the source of the laterization process in the region was the ultrabasic igneous rocks. The lateritic material moved by superficial transfer was accumulated on sandstone, claystone, siltstone, and limestone and in karstic cavities; then, it formed karstic bauxite (kaolinitic and bauxite) of different classifications due to the effect of metamorphism.

Keywords: *karstic bauxite, lateritic bauxite, geochemistry, mineralogy, petrography, multivariate statistics*

1. Introduction

The study area, the Sutlegen region, is located within the Western Taurus belt (Fig. 1). The geochemical explanation of the elemental relationships that play a role in the formation of bauxites in the region can be given as a problem formulation within the scope of the study. The trace and rare earth elements' relationships were examined using multivariate statistical methods to determine the mineralogical and petrographic properties of bauxite samples and paleo-climatic conditions. When the metamorphism conditions are met, the clay layers get enriched in metallic formations such as alumina and get depleted in silica. In the next stage after this formation, bauxite minerals such as gibbsite, boehmite, or diaspore are enriched. Thus, the concentrations of precious metals such as Al, Fe, and Ti increase [1]-[7]. The chemical content of bauxite is composed of high levels of major, trace, and REE elements (Ti, P, Zr, Nb, Ni, Cr, Co, V, Ga, U, Sc), and particularly Al metal [1], [4], [5], [7]-[16].

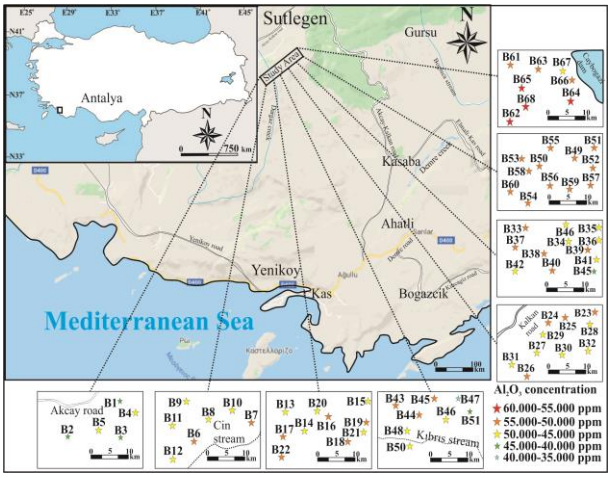

Figure 1. Site location map of the study area, sample numbers, and aluminum anomaly

Received: 28 June 2021. Accepted: 30 August 2021. Available online: 22 September 2021

Published by the Dnipro University of Technology on behalf of Mining of Mineral Deposits. ISSN 2415-3443 (Online) | ISSN 2415-3435 (Print)

The behavior of mobile elements during the formation of bauxite indicates the intensity of chemical weathering. The physicochemical conditions (Eh-pH, paleoclimatic properties, etc.) during the formation of the ore are determined using these mobile elements [17]-[21].

Three types of bauxite classifications have been adopted in the international literature: lateritic bauxite, karstic bauxite, and Tikhvin-type (sedimentary) bauxite [22]-[24]. Although lateritic type bauxites are rich in gibbsite minerals, aluminosilicate rocks are the source rock in their formation [3], [25]. The relationship between the karstic bauxites and the parent rock can be either allochthonous or autochthonous [7]. Therefore, the discussions on the determination of the geological genesis of the karstic bauxite deposits have still been going on. There are several studies on karst-type bauxite deposits in the literature. In a study on karst-type bauxite deposits in north-western Iran, the bauxite ore, which was formed within the dolomitic limestones in lens form, was investigated in terms of its mineralogical and petrographic characteristics. The XRD and SEM-EDS analyses revealed that the major minerals of bauxite were diaspore and hematite, while the mineralogical components of clay lenses were kaolinite and montmorillonite. Also, the analyses revealed that the metal content consisted of Ni, Cr, Co, V, Fe, Nb, Ga, Ta, Th, Hf, and Zr besides Al. In the model proposed for bauxite formation in Iran, it was considered that alkali and alkaline earth metals were depleted at the top of the profile under acidic environment conditions; also, with the deepening of the profile, the acidic character of the environment changed, thus, the environment was enriched in metallic bauxitic minerals and elements [7]. The major mineral composition of the karst-type clay bauxite deposit in Semirom in the Himalaya region was found to be diaspore, boehmite, kaolinite, and hematite [4]. The elements of Cr, Co, Ni, Ga, and Th were found to have an increasing concentration in the bauxitic material [4]. In the geochemical genesis study on the bauxite deposit in the Henan region in China, the ore formed on the karstified carbonate series was found to be rich in Li, B, Sc, V, Ga, Zr, Nb, W, and total REE. In the research, it was observed that the behavior of the Li, B, V, Cr, and Ga elements increased directly proportional to K_2O and SiO_2; as a result, the increase in the clay minerals in the environment was associated with bauxite formations [6].

The objectives of the study are listed as follows; to learn the major, trace and rare earth elemental concentrations of bauxite in the region, to determine the connection between regional geology and bauxite formations, to understand the bauxite formation environment conditions, to determine the types and geological genesis of bauxite occurrences in the region.

2. Methods

The Sutlegen region, the study area, is located 37 km north of the Mediterranean coastline and 168 km from Antalya between Kalkan (Kas) and Elmali districts. Sixty-eight surface samples were taken from the Sutlegen region. The samples were brought to Akdeniz University's "Ore Deposits Laboratory" and prepared for analysis.

Five samples were analyzed by optical microscopy imaging methods, four samples were analyzed by X-ray diffraction (XRD), sixty-eight surface samples were analyzed by X-ray fluorescence (XRF), and seventeen samples were analyzed by inductively coupled plasma-mass spectrometry (ICP-MS). The petrographic analyses were carried out in accordance with the procedures detailed in the studies [26]. ICP-MS analysis was carried out at the Mineralogy-Petrography Research Laboratory of the General Directorate of Mineral Research and Exploration, XRD (BRUKER, D8 ADVANCE) and optical microscope imaging were carried out at the Mineral Deposits Laboratory of Istanbul Technical University, and XRF (Rigaku, NEX-CG) analyses were performed at the XRF Laboratory of Akdeniz University. In the XRF spectroscopy method, geological materials are exposed to high-energy radiation, thus, the electrons in their internal orbits are removed. At this stage, fluorescence radiation occurs during electron detachment, and it reflects the characteristics of each different element. The device distinguishes the fluorescence of the elements known in the literature and performs both qualitative and quantitative analyses according to their intensity [27]. The REE and trace elements in rock samples are analyzed using the ICP-MS device after a difficult sample preparation process. Hydrofluoric acid (HF) and similar strong acids are used to dissolve geological samples [28]. The acid better penetrates the sample by heating, and the rock is expected to show complete dissolution. The prepared sample solution is atomized using high flame technology [28].

2.1. Regional geology of the study area and geology of the Sutlegen bauxite deposits

In the study area, there are allochthonous (Yesilbarak nappe) and autochthonous (Elmali Formation, Quaternary alluvium, and hillside rubble) rock units showing various stratigraphic and structural characteristics. The Katran Mountain region, where the bauxites of the study area are observed, is represented by the Beydagları autochthonous (Fig. 2a, b).

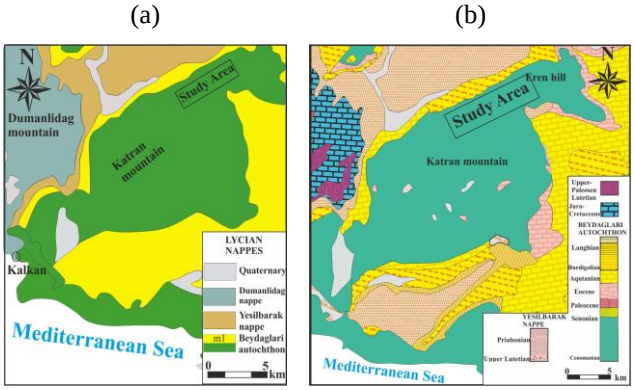

Figure 2. Geological map: (a) structural units map of the study area; (b) 1/250.000-scale geologic map, P23 sheet (edited version of the raster map of MTA 1:250000 Fethiye P23 sheet) [29]

In the study area, the formations can be ordered from the oldest to the youngest as the Beydaglari formation belonging to the Upper Cretaceous period in the Mesozoic era, the Susuzdag formation belonging to the Eocene period in the Cenozoic era, and the Sinekci formation (Gumuce member at the bottom and Caybogazi member at the top) belonging to the Burdigalian period in the Miocene era. The Beydaglari autochthonous is overlain by the Kasaba Formation belonging to the Upper Burdigalian-Lower Langhian period in the Miocene era. The Elmali formation, which was formed in the Eocene-Miocene era, is tectonically associated with the Yesilbarak nappe, which also includes the Upper Lutetian-Lower Burdigalian rocks. (Fig. 3) [30]-[34].

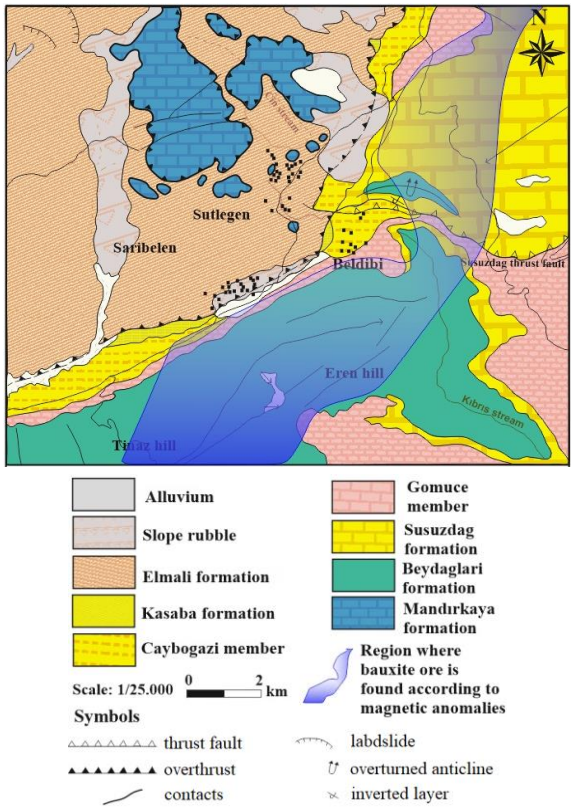

Figure 3. Geologic map of the study area and bauxite area [35]-[37] (edited version of the raster map of MTA 1:100000 Fethiye M9 sheet)

Due to the transgression as a result of the epeirogenic movement, members of the Sinekci formation (Gomuce member, Caybogazi member) and Kasaba formation rocks were deposited on the Beydaglari autochthonous. Mandirkaya formation, as a geological unit observed in the Sutlegen region, is seen in the vicinity of Yaylacik Hill, and it seems like a massive rich in neritic carbonates [30]-[39].

The Beydaglari formation consists of neritic limestone, dolomite, dolomitic limestone units and forms the upper boundary of bauxite ore. Susuzdag formation consists of neritic limestones. The Gomuce member of the Sinekci formation consists of algal limestones and the Caybogazi member of the Sinekci formation consists of clays on the top. Kasaba formation consists of coarse-grained clastic conglomerate, sandstone, claystone, and siltstones.

In the intermediate zone (Yesilbarak Nappe), Elmali formation consists of limestone, intermediate-level sandstone, mudstone, and shales. As one of the cover units, alluvium generally consists of yellowish, poorly sorted, poorly consolidated conglomerates, sand, and mudstone levels. Considering the suitable paleokarstic topography of the area, which is bounded by limestones at the top and bottom, the limestones were formed in a discordant structure. The Elmali formation, which is the exposure surface of the region, forms the lower boundary of bauxite formations that occurred in the depths of the formation in later periods (Fig. 4).

The color scale of the bauxitic profile from the bottom to the top was observed to range from light brown to dark brown and dark smoked. It was also observed that they showed oolitic and pisolitic characteristics in round grained structure as a textural feature.

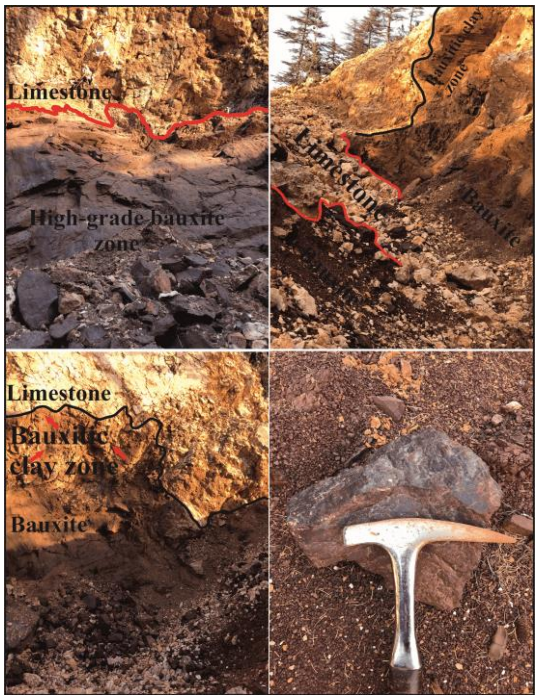

Figure 4. A bauxite profile sampled in the Sutlegen Paleokarstic valley

3. Results and discussion

3.1. Mineralogy

The spectra of the semi-quantitatively measured XRD analysis revealed the mineralogical composition of bauxite. The Sutlegen bauxite was found to constitute the dominant mineral phases of boehmite (56.34-49.04 wt%), kaolinite (12.20-9.89 wt%), hematite (15.17-7.72 wt%), gibbsite (12.18-7.17 wt%), goethite (4.07-1.56 wt%), and anatase (13.11-6.21 wt%). On the other hand, anorthite, quartz, and chamosite are the minor mineral phases in the content (Table 1 and Fig. 5). According to the proportions of mineral content, ore paragenesis can be listed as follows:

boehmite > kaolinite > hematite > gibbsite > goethite > anatase > anorthite > quartz > chamosite.

Table 1. XRD results of bauxite samples

Minerals in bauxite samples	Invention formulas	B16	B27	B32	B34
Boehmite	Al(OH)	55.76	49.04	49.16	56.34
Kaolinite	$Al_2Si_2O_5(OH)_4$	10.21	10.79	12.20	9.89
Hematite	α-Fe_2O_3	10.15	15.17	14.64	7.72
Gibbsite (hidrarjilit)	$Al(OH)_3$	12.18	9.74	7.17	7.92
Goethite	$Fe^{3+}O(OH)$	3.77	2.61	4.07	1.56
Anatase	TiO_2	6.21	7.41	10.49	13.11
Anorthite	$(Ca.Ni)(Si.Al)_4O_8$	0	3.72	0	3.42
Quartz	SiO_2	0	1.48	2.23	0
Chamosite	(Fe Al Mg Mn_6 (Si Al)$_4O_{10}(OH)_8$	1.67	0	0	0
Total		100	100	100	100

Bauxite samples have high boehmite and kaolinite content. Considering the tropical climate conditions in the formation environment of bauxite, the boehmite mineral was formed as a result of the destruction of kaolinite/dehydration reactions [4], [18], [40].

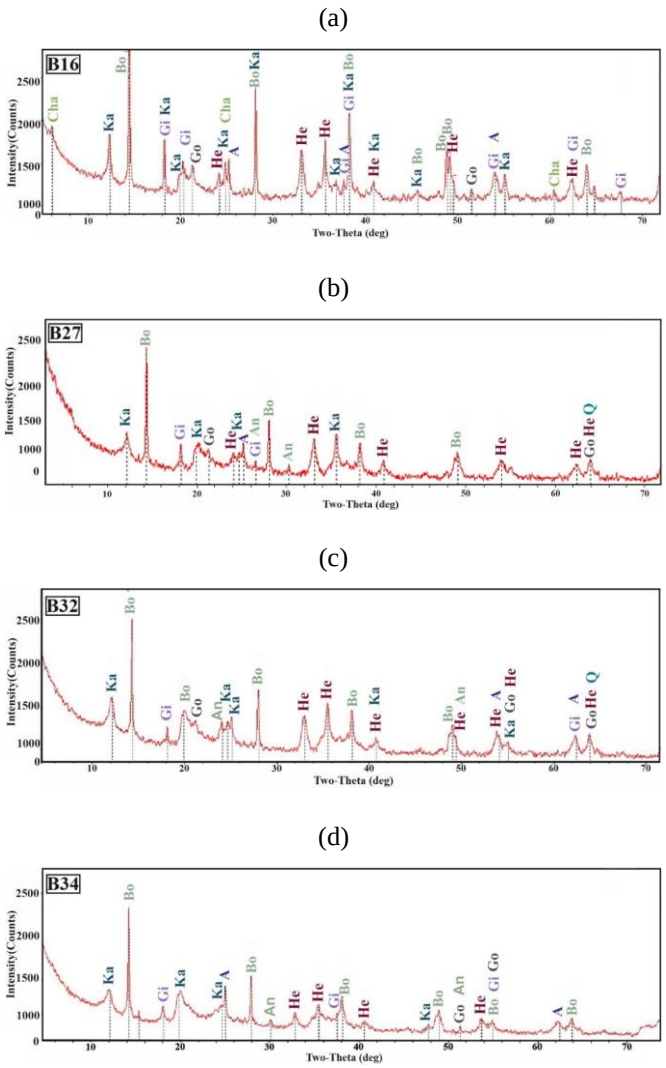

Figure 5. XRD patterns of the Sutlegen bauxite profile: (a) B16; (b) B27; (c) B32; (d) B34; Bo – boehmite; Ka – kaolinite; He – hematite; Gi – Gibbsite; Go – goethite; A – anatase; An – anorthite; Q – quartz; Cha – chamosite)

The bauxite matrix is composed of clay and Fe-oxide/hydroxide minerals. While the brightest mineral observed in the cross-sections (Fig. 6a-f) is hematite, goethite is the second brightest mineral. Goethite mineral has iron content. In the cross-sections, hematite mineral is observed to be disseminated. The minerals providing cloudy internal reflections in the cross-sections are boehmite (Fig. 6b, c, d, f). The order of the minerals formed when bauxites undergo metamorphism is as follows: gibbsite, boehmite, and diaspore. The mineral dehydrates as it goes from gibbsite to diaspore.

3.1.1. Major elements geochemistry

Ore content was found to be Al_2O_3 (60-35.2 wt%), SiO_2 (39.5-0.2 wt%), Fe_2O_3 (48.4-19.5 wt%), TiO_2 (36.9-16 wt%), P_2O_5 (0.5-0.1 wt%) (Table 2). The fact that SiO_2 and Fe_2O_3 compounds have the highest concentrations following Al_2O_3 in the Sutlegen bauxite is associated with the mineralogical change. Changes in the chemical composition are under the control of the mineralogy [4], [7], [41], [42]. While the SiO_2 value increases depending on the kaolinite and anorthite minerals, the Fe_2O_3 value changes by the increase in the hematite and goethite minerals.

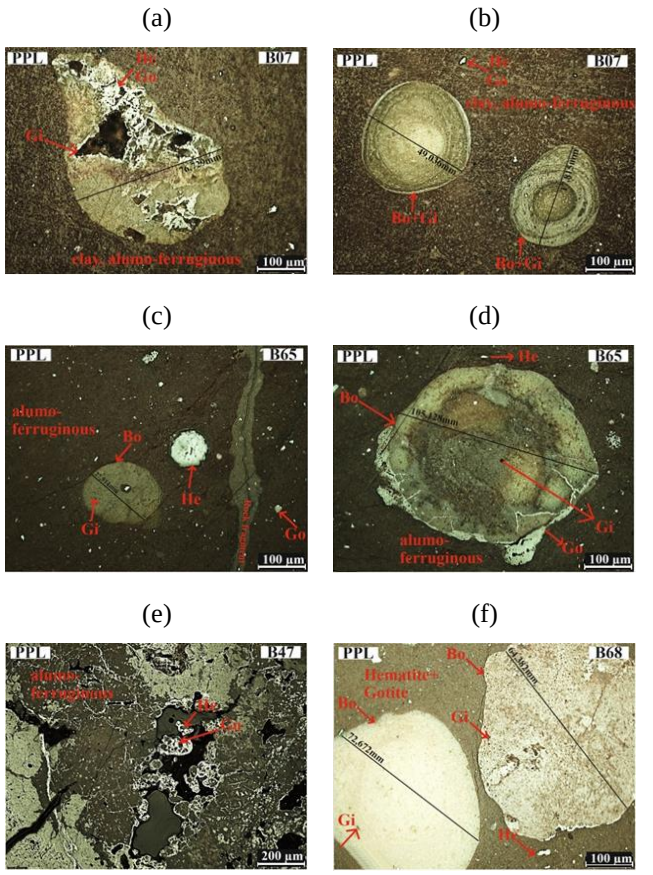

Figure 6. Microphotographs of the Sutlegen bauxites: (a) sample B07, clay with an alumo-ferruginous matrix with a pisolitic texture of He + Go + Gi; (b) sample B07, clay with an alumo-ferruginous matrix with an oolitic texture of Bo + Gi; (c) sample B65 with an alumo-ferruginous matrix with an oolitic texture of Bo + Gi, He, Go; (d) sample B65 with an alumo-ferruginous matrix with a pisolitic texture of Bo + Gi, He, Go; (e) sample B47 with an alumo-ferruginous matrix with a pisolitic texture of He + Go; (f) sample B68 with He + Go matrix composition with a pisolitic texture Bo + Gi, He, Gi; PPL – single nicol; Bo – Bohmite; Gi – Gibbsite; He – Hematite; Go – Goethite

Table 2. Descriptive statistics of major element oxides of the Sutlegen bauxites (ppm)

	Min	Max	Mean	Median	Mode	Variance	Range
Al_2O_3	352000	600000	503279.41	504000	480000	1404353600	248000
SiO_2	23000	395000	255852.94	259500	311000	4288425812	372000
Fe_2O_3	19500	484000	193730.88	189500	174000	3092524256	464500
TiO_2	16000	369000	38257.35	28100	28100	2515058303	353000
MgO	0	4990	1516.62	0	0	3906294.36	4990
P_2O_5	1230	5710	2180	1990	1350	1021262.69	4480
SO_3	289	1980	5419	493.5	332	62.542.231	1691
K_2O	0	4470	1595.18	1205	0	1634862.54	4470
CaO	978	4310	2257.62	2150	1730	394.255.792	3332

The differences in SiO_2 and Al_2O_3 values in ore samples are associated with laterization reactions during bauxite formation [7]. According to the Al_2O_3-SiO_2-Fe_2O_3 triangular diagram (after [43]) which shows the degree of lateritization, the ferritic bauxite sample B55 ($B55_{SiO2}$: 23000 ppm) has the lowest SiO_2 content and shows the strongest laterization among the Sutlegen samples. The K_2O, MgO, and CaO, which are classified as alkaline and alkaline earth elements, have low concentrations. They show mobile element behavior during the formation of bauxite and deplete easily in the environment [44], [45].

3.1.2. Trace elements

The trace element contents of the Sutlegen bauxites are listed in descending order as follows: Mn (6030-111 ppm) > V (1500-0 ppm) > Sr (1140-107 ppm) > Co (933-247 ppm) > Cr (913-319 ppm) > Ni (691-0 ppm) > Cu (606-51.4 ppm) > Zn (528-168 ppm) > Y (458-57.5 ppm) > Ce (363-0 ppm) > La (269-0 ppm) > Pb (262-65 ppm) > As (220-0 ppm) > Ba (209-0 ppm) > Nb (169-0 ppm) > Th (106-0 ppm) > Ga (73.5-39.4 ppm) > Sn (57.1-28.2 ppm) > Hf (59.5-0 ppm) > Rb (51.7-0 ppm) > Sb (38.8-0 ppm) > Ta (37.2-0 ppm) > W (29.2-0 ppm) > U (27.1-0 ppm) > Te (22.1-0 ppm) > Hg (20.6- 0 ppm) > Au (19.7-0 ppm) > Cd (18-0 ppm) > Pt (17.7-0 ppm) > Ir (17.5-0 ppm) > Bi (15.4-0 ppm) > Br (12-0 ppm) > In (11.8-7.06 ppm) > TI (8.8-0 ppm) > Se (5.9-0 ppm) > Ge (7.29-0 ppm) (Table 3). It is known that karst-type bauxite formations around the world have a Ga element content of about 58 ppm [6], [46]. The distribution of the Sutlegen bauxites is similar to the Ga element behavior of the karst-type bauxites in the world [47].

Table 3. Descriptive statistics of trace element concentrations of the Sutlegen bauxites (ppm)

	Min	Max	Mean	Median	Mode	Variance	Range
Mn	1110	60300	9704	6300	535	12365430	59190
V	0	15000	828.75	825.5	0	1088850	15000
Sr	3190	11400	357.59	2740	119	64109.1	10330
Co	2470	9330	470.68	456.5	4550	12437.6	6860
Cr	1070	11400	565.79	5440	5020	12911.4	5940
Ni	0	6910	338.72	3350	245	9465.1	6910
Cu	1680	5280	1306	1050	1070	5968.37	5550
Zn	0	3630	283.34	273.5	191	5341.48	3600
Y	580	4580	131.28	109.5	1030	6400.65	4010
Ce	510	6060	220.35	2280	0	5945.69	3630
La	0	1690	100.85	1140	0	72736	2690
Pb	650	2620	101.42	95.55	1020	6875920	1970
As	0	2690	86.83	78.35	72	1944.39	2200
Ba	0	2200	55.19	66.95	0	3161.95	2090
Nb	390	740	116.84	116.5	1350	6474080	1690
Th	0	1060	57.63	57.25	00	2589620	1060
Ga	0	2090	60.46	60.8	570	391810	340
Sn	280	570	429	42.2	40	240250	290
Hf	0	600	35.47	35.7	0	1900390	600
Zn	0	520	283.34	273.5	191	5341.48	3600
Rb	0	270	19.91	439360	12	1950470	520
Sb	0	290	418520	0	0	1038690	390
Ta	0	200	439230	0	0	742690	370
W	0	390	361300	439670	0	907980	290
U	0	180	13.84	14.25	0	294220	270
Te	0	220	165580	0	0	530450	220
Hg	0	210	187190	0	0	260890	210
Au	0	370	174110	459310	0	179480	200
Cd	0	90	0.26	0	0	47650	180
Pt	0	150	441720	265120	0	352910	180
Ir	0	120	440440	0	0	152450	180
Bi	0	180	262990	0	0	116530	150
Br	0	60	135160	0	0	56480	120
In	0	120	0.28	0	0	27440	120
TI	0	180	284910	0	0	81660	90
Se	0	70	0.64	0	0	27920	60
Ge	1110	60300	0.18	0	0	10820	70

3.1.3. REE geochemistry

Another chemical composition that contributes to the formation of bauxite is the rare earth elements. The rare earth element contents of a total of 17 samples were determined by ICP-MS analysis. These elements are listed according to their averages in descending order as follows: Ce (105.20-5.20 ppm) > Nd (70-3.70 ppm) > Sc (36.60-10.10 ppm) > Dy (23.6-1.10 ppm) > La (22.50-2.70 ppm) > Gd (18.80-0.90 ppm) > Sm (18.60-1.10 ppm) > Er (13.10-0.6 ppm) > Yb (11.6-0.6 ppm) > Pr (11.80-0.70 ppm) > Ho (5-0.20 ppm) > Eu (3.90-0.20 ppm) > Tb (3.50-0.20 ppm) > Tm (0.3-0.1 ppm) > Lu (0.3-0.1 ppm). Descriptive statistics of the results are given in Table 4. ∑REE, ∑LREE (La-Sm), ∑HREE (Gd-Lu), and ∑LREE/HREE values and descriptive statistics of these results are given in Table 5.

Table 4. Descriptive statistics of rare earth elements (REE) data of the Sutlegen bauxites (ppm)

	Min	Max	Mean	Median	Mode	Variance	Range
Ce	439520	105.10	4060590	39.2	5.20	1066.89	99.9
Nd	256280	700	2683530	439090	64.1	5593210	66.3
Sc	441140	36.60	2175880	440330	10.10	414760	439770
Dy	441050	23.60	1207060	439040	1.10	534860	439730
La	256000	22.50	1068240	438990	2.70	387180	440620
Gd	0.90	18.80	921760	438390	0.90	393130	440910
Sm	441050	18.60	832940	439280	1.10	382750	439680
Er	0.60	441170	683530	440810	439290	153640	439630
Yb	0.60	222210	659410	438370	7.10^{a}	114990	110
Pr	0.70	295260	445290	439240	0.9	155880	438410
Ho	0.20	50	251760	440760	0.80	22490	440470
Eu	0.20	329330	197650	440130	0.80	18240	440150
Tb	0.20	183230	440440	20	0.50	12990	438930
Tm	< 0.1	0.3	111180	438310	0.40	0.401	20
Lu	< 0.1	0.3	102350	438310	0.60	0.278	440130

Table 5. The results of ΣREE, ΣLREE, ΣHREE and ΣLREE/ΣHREE calculations of the bauxite samples in the study area

	∑REE	∑LREE	∑HREE	∑LREE/∑HREE
B3	295.9	185.6	103.4	1794.00
B8	209.9	115.4	93.6	12329.00
B19	184.6	88.7	101.6	0.87303
B55	86.3	44069	71.4	0.3753501
B62	44038	43902	16.00	0.76875
B21	50.8	43967	41.9	0.3937947
B33	176.1	105	72.7	14442916
B42	54.6	4396	40.9	0.4523227
B44	142.2	82.6	63.1	13090333
B50	97.6	56.1	44.9	12494432
B49	97.4	55.2	44	12545455
B37	206	95.5	111	0.85
B64	289.1	203.4	80.1	25393258
B66	297.5	197.8	93.4	2117773
B52	100.6	43980	79.3	0.372005
B30	44.5	440670	43944	10598291
B9	176.2	90.1	83.7	10764636
Mean	14920	82576	685117	11277575
Std. Dvd.	8981668	6347113	28885240	0.6123101

It was determined that ∑REE values ranged between 297.5-26.7 ppm, ∑LREE values ranged between 203.4-12.3 ppm, ∑HREE values ranged between 111.3-16 ppm, and ∑LREE/HREE values ranged between 2.53-0.37 ppm. The ∑LREE content of the Sutlegen bauxites was observed to be higher than ∑HREE content. Bauxites enriched in ∑LREE are affected by the change in the content of Ce, which is one of the HREE elements [4]. In karst-type bauxite deposits, the ∑HREE concentrations show lower distribution compared to ∑LREE concentrations [4].

3.1.4. Laterization and classification of bauxites

The Al_2O_3-SiO_2-Fe_2O_3 diagrams are preferred to determine the degree of laterization of bauxite ore, to control the minerals during lateritization, and to classify the baux-

ite [44], [48]-[54]. According to the Al_2O_3-SiO_2-Fe_2O_3 diagram, the samples were observed to have the following four groups: kaolinitic bauxite, laterite, bauxite, and ferritic bauxite. While most of the samples fell into the bauxite group, the B55 sample was classified as ferritic bauxite; B47 and B51 samples were classified as laterite; and B31 and B38 samples were classified as kaolinitic bauxite (Fig. 7a).

According to the triangular diagram indicating the degree of lateritization, the samples showed medium and strong laterization. The B55 sample, which was classified as ferritic bauxite, showed the strongest laterization (Fig. 7b). Other bauxite samples in the triangular diagram fell into the range between kaolinite and bauxite (Fig. 7c). In the diagram regarding the geochemical formation mechanism of bauxite, bauxite samples revealed that they were formed as a result of deferruginization in the environment (Fig. 7d). In the diagram that revealed the environmental conditions of bauxite, the samples were mostly seen in the range between bauxite and clayey bauxite. However, the samples of B42 and B51 were identified as high-iron bauxite.

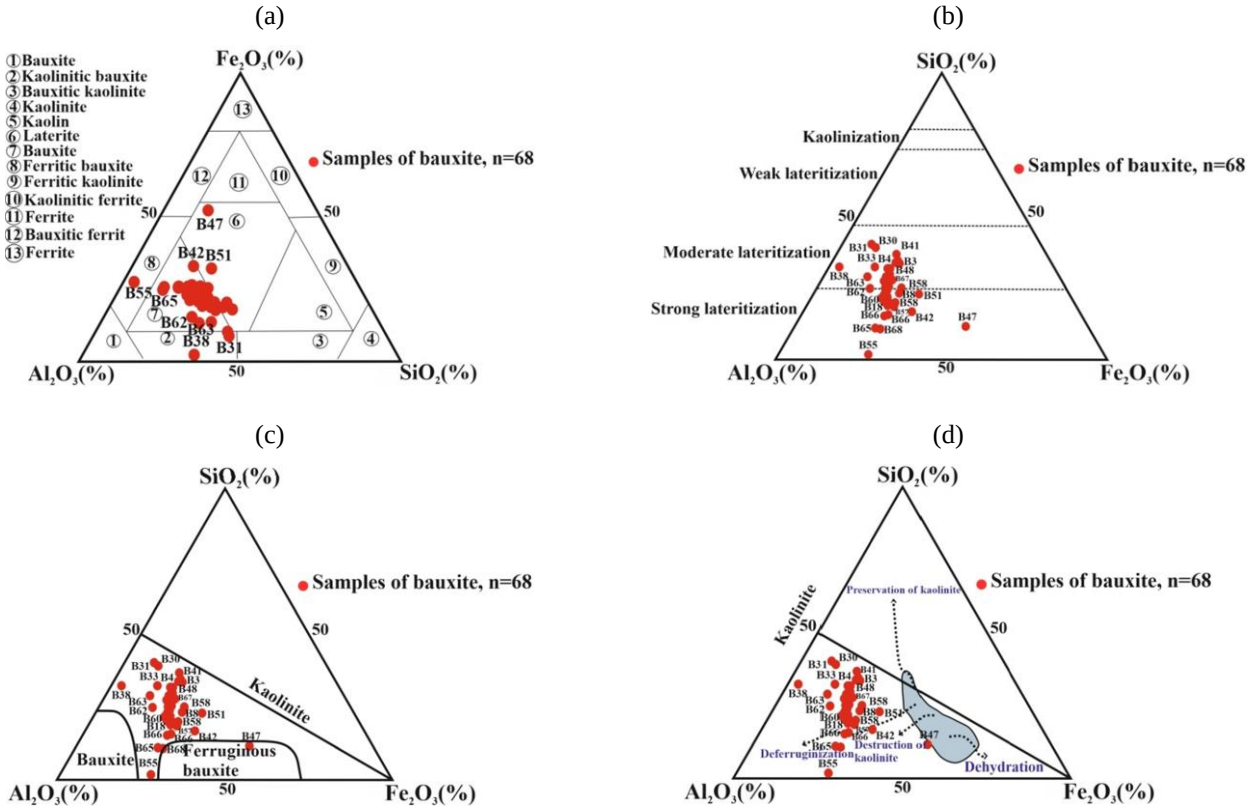

Figure 7. SiO_2-Al_2O_3-Fe_2O_3 triangle diagram of the Sutlegen bauxites: (a) Fe_2O_3-Al_2O_3-SiO_2 triangular diagram showing the mineralogical classification [48]; (b) Al_2O_3-SiO_2-Fe_2O_3 triangular diagram showing the degree of lateritization [43]; (c) Al_2O_3-SiO_2-Fe_2O_3 triangular diagram showing the bauxite classification [51]; (d) geochemical ways of bauxite formation mechanism [53]

Normalized spider diagrams can be used to determine whether the elements are enriched or impoverished in bauxite [26], [55]. The Upper Continental Crust (UCC)-normalized trace element pattern of ferritic bauxite and kaolinitic bauxite shows depletion in Ti, Sr, Ba, and Rb and enrichment in Hf, Ce, and K. In bauxite samples, ferritic bauxite and kaolinitic bauxite are similar to each other except for their Ti values. In laterite, the elements of Sr, Nb, Th, and Ba show depletion, while Y, La, and K show enrichment (Fig. 8a, b).

In Table 6, several properties such as major elements, total REE content, paleoclimatic conditions, and degree of laterization observed in the karst-type bauxite deposits in the world literature were compared to those of the Sutlegen bauxite deposit. The average Al_2O_3 content (60-35.20 wt%) of the bauxite samples is higher than that of the bauxite samples in the world literature. TiO_2/Al_2O_3 values are greater than other karst-type samples in the world except for Jamnagar district bauxites (Gujarat, India) and Apulian bauxites (southern Italy). In terms of total REE, the bauxite samples show more depletion than other karst-type samples.

3.2. Multivariate statistical analysis

3.2.1. Cluster analysis

Cluster analysis was performed to determine the classification of the chemical contents of bauxite samples [58] (Fig. 9). According to the groups obtained by the dendrogram using the chemical contents (major and trace elements), bauxite samples were grouped under three groups. The similar characteristics of the geochemical behaviors of these groups were revealed. According to the Aleva (1994) diagram, the samples constituting Group 1, except for the sample of B33, fall into the bauxite area. The sample of B33 showed kaolinitic bauxite properties. The Al_2O_3 concentrations of the following samples with close relationships ranged between 54-49 wt%: B34, B35, B5, B36, B20, B21, B48, B32, B33, B12, B14, B46, B50, B9, B10, B28, B11, B13, B27, and B15. All major and trace element concentrations were observed to be similar except for the concentrations of the major element of MgO and the trace elements of Br, Se, Sb, Te, Ba, Hf, Ta, W, Pt, and Th. The geochemical behavior of the samples of B1, B2, B3, and B41, which were externally connected to this group, ranged between 47-43 wt% in terms of Al_2O_3.

Table 6. Comparison of certain properties of the Sutlegen bauxite deposit with samples from the literature (elemental composition properties, ΣREE degree of weathering, mineralogical classification and source rock)

Locations of bauxite occurrences	Al_2O_3 (wt %)	TiO_2/Al_2O_3	Sm/Nd	ΣREE (ppm)	Degree of weathering	Mineralogical classification	Parent rock
Lower Cretaceous (NE Spain) [21][21]	26.34-60.88	0.4-0.7	0.14-0.36	78.89-815.75	Weak to strong	BK, KB, B, L	Mafic argillaceous sediments
Northern Guizhou Province (China) [44]	27.67-76.35	0.1-0.5	0.12-0.51	13.50-8470	Weak to strong	BK, KB, B	Shale and limestone derived from basic rocks
Jamnagar district (Gujarat. India [18]	34.74-57.24	0.7-0.14	0.14-0.38	590-4280	Weak to strong	FB, B, KB	Trachyte/andesite
Apulian bauxites (southern Italy) [9]	39.38-58.46	0.8-0.10	0.18-0.23	152.20-1167.40	Strong	B	Distal magmatic materials and continental clastic
The Sutlegen bauxites (SW, Turkey) [This study]	60-35.2	0.70-0.3	0.57-0.24	297.5-26.7	Moderate to strong	B, KB, FB, L	Laterite derived from ultrabasic and karstic

FB = ferritic bauxite, KB = kaolinitic bauxite, BK = bauxitic kaolinite, B = bauxite, L = laterite

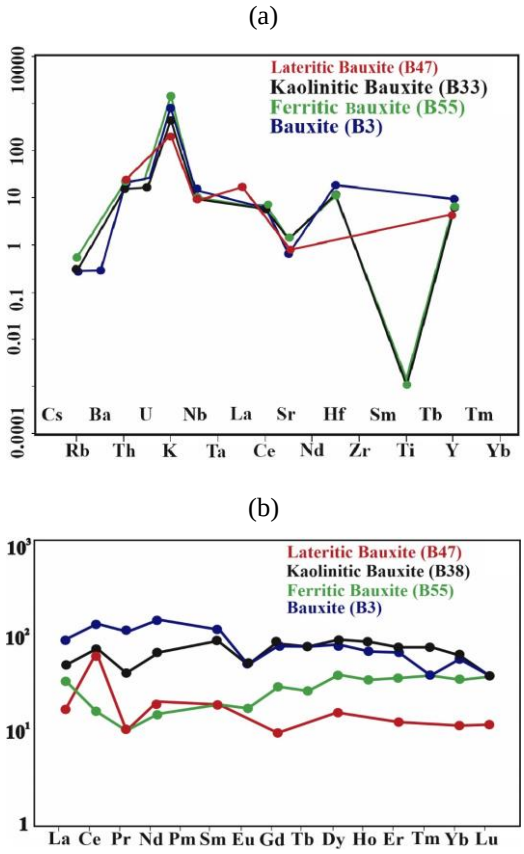

Figure 8. Spider diagrams: (a) chondrite normalized spider diagram of samples (normalization values [56]); (b) the Upper Continental Crust (UCC)-normalized spider diagram of the samples (UCC values were received from [56], [57])

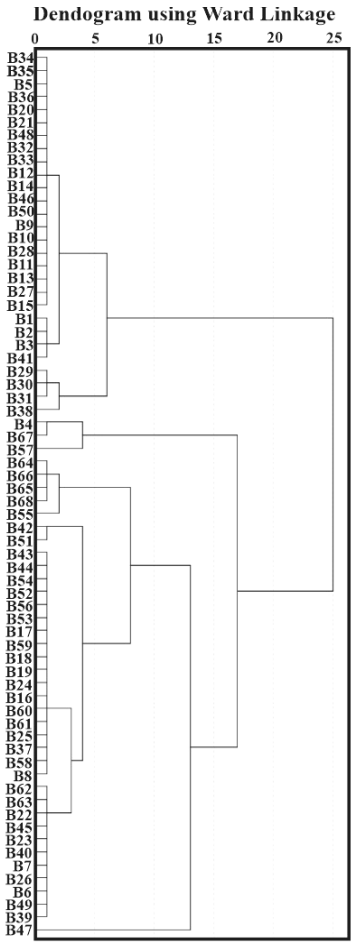

Figure 9. Dendrogram of the Sutlegen bauxite samples

Their Al_2O_3 values are lower than that of the group they joined. They show the characteristics of the group they join in terms of trace element concentration. B29, B30, B31, and B38 are the last samples that joined Group 1. Their geochemical properties showed lower Al_2O_3 concentrations (50-47 wt%) compared to the group they joined. Their major element contents and trace element contents showed similar characteristics with the group they joined. Group 2 consists of the bauxite samples of B4, B67, and B57. The Aleva (1994) diagram revealed that the samples of B4 and B57 were classified as bauxite, and the sample of B67 was classified as lateritic bauxite.

The most important reason why these samples differ from other groups is that they have the highest TiO_2 values among bauxites (36-18 wt%). On the other hand, their Al_2O_3 concentrations range between 52-47 wt%. They were observed to have similar geochemical properties except for the major element of MgO and the trace elements of Br, W, Hf, Cd, and Sb. The following samples constitute Group 3: B43, B44, B54, B52, B56, B53, B17, B59, B18, B19, B24, B16, B60, B61, B25, B37, B58, B8, B62, B63, B22, B45, B23, B40, B7, B26, B6, B49, and B39. According to their geochemical behaviors, their Al_2O_3 contents range between 56-47 wt%, and their TiO_2 values range between 3.8-2.4 wt%.

According to the Aleva (1994) diagram, these samples were classified as bauxite. These samples show similar characteristic elemental properties among themselves, except for the major element of MgO, and trace elements of Br, Se, Sb, Te, Ba, Ta, W, and Pt. The reason why this group differs from Group 1 is that it shows relatively higher concentrations of Al_2O_3 and TiO_2. The codes of the samples that externally joined to Group 3 are B42, B51, B64, B66, B65, B68, and B55. The Aleva (1994) diagram reveals that the samples of B42 and B51 are lateritic bauxite, the sample of B55 is ferritic bauxite, and the samples of B64, B66, and B68 are bauxite. The reason why they are similar to Group 3 is that most major and trace element contents have similar properties. While Al_2O_3 values range between 60-43 wt%, B65, which has the highest Al_2O_3 concentration among all bauxite samples, is also listed in this group. On the other hand, this group, which shows high concentrations of Al_2O_3, has the lowest values of SiO_2 among bauxite samples (23-2.3 wt%).

The sample of B55, which is classified as ferritic bauxite, has the lowest SiO_2 value among all the samples (2.3 wt%). According to the Aleva (1994) diagram, the sample of B47, which is the last sample that externally and remotely joined to the group, is classified as lateritic bauxite. Also, the sample of B47 shows the lowest Al_2O_3 concentration among all the samples (35.2 wt%).

Moreover, the sample of B47 shows the highest Fe_2O_3 value (48.4 wt%) among all samples. The sample of B47 joins Group 3 because it shows similar levels of trace element concentrations (V, Cr, Co, Ni, Cu, Zn, Ga, Sr, Y, Nb, Sn, Te, Th, and Pb). The following general conclusion can be drawn from the dendrogram analysis: In terms of their geochemical content, the samples classified as kaolinitic bauxite show similar characteristics with the samples classified as bauxite. However, the samples classified as lateritic bauxite show similar characteristics with both bauxite and ferritic bauxite samples.

3.3. Results of weathering indices of bauxites

The CaO^* value in the CIA (Chemical Alteration Index), CIW (Chemical Index of Weathering), and WIP (Weathering Index of Parker) calculations must be calculated at first because it contains the CaO value of silicate minerals [59], [60]. The CIA and CIW values between 80-100 indicate intense chemical alteration [61], [62]. The CIA values of bauxite samples were found to range between 99-100. The values of the weathering index of Parker were found to range between 0.36-5.84.

The WIP values of 9 samples from the Sutlegen region range between 5.84-5.10, 4 samples' WIP values range between 4.74-4.01, 5 samples' WIP values range between 3.8-3.09, 13 samples' WIP values range between 2.85-2.11, 24 samples' WIP values range between 1.83-1.04, and 13 WIP values range between 0.86-0.36. The largest range of the weathering index of Parker is observed to be between 1.83-1.04 (in 24 samples) in the Sutlegen bauxite samples. The average WIP value to represent the region was calculated as 2.34.

Ruxton ratio (R) defines the silica-alumina ratio of the bauxites [63]. The R values of the samples were observed to be very close to the optimum weathering limit. The average value of R was found to be 0.51. The sample of B41 was found to have the highest value of R in the region, while the sample of B55 showed the lowest value of R.

The WIP index and R ratio are used to understand the weathering rate of Al_2O_3. They indicate through which processes the bauxite samples of the kaolinitic bauxite, ferritic bauxite, and bauxite classification have formed since the laterization period. It was observed that the WIP index and R ratio changed inversely proportional to the increase in Al_2O_3 value.

The WIP index reaches the highest values in areas where the process of laterization begins and lateritic bauxite forms. It declines in the areas where kaolinitic bauxite is observed. On the other hand, it has the lowest values in the ferritic bauxite and bauxite classification areas (Fig. 10a). Also, the R ratio is expected to decrease in line with the laterization and kaolinization processes. In bauxite formation processes, the Al_2O_3 increase in the environment will be inversely proportional to the R ratio. Lateritic bauxite samples are observed to show the highest R ratio. However, this ratio tends to decrease towards the kaolinitic bauxite classification area. Besides, the samples in the ferritic bauxite and bauxite classifications have the lowest R values (Fig. 10b).

(a)

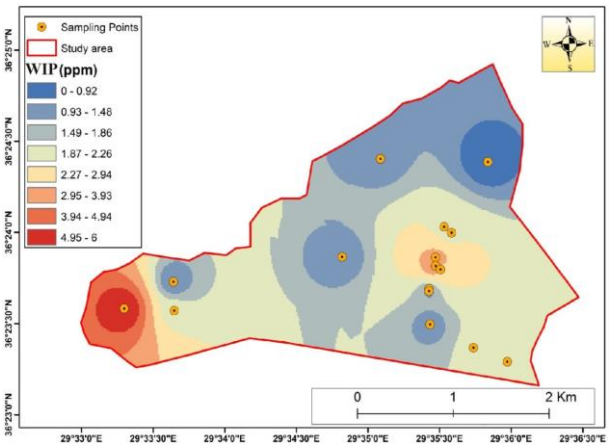

(b)

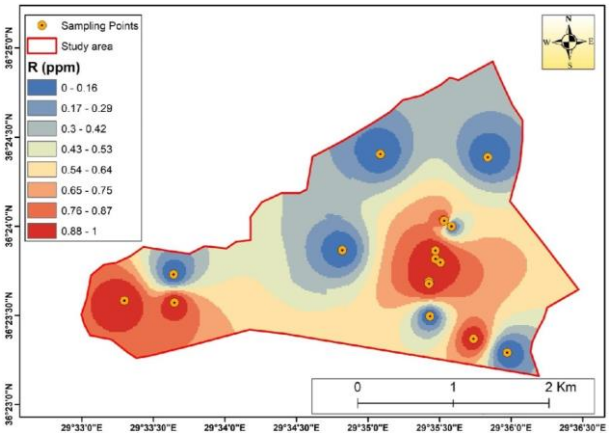

Figure 10. Distribution maps: (a) distribution map of WIP; (b) distribution map of R

Considering the spatial distribution maps, it can be deduced that Al_2O_3, Fe_2O_3, and TiO_2 concentrations change inversely proportional to the chemical decomposition reactions of the Sutlegen bauxites. Considering the spatial distribution of WIP and R index calculations, it can be said that the increase in the Al_2O_3 concentration resulted in a decrease in the ore formed in the region. The WIP and R values of lateritic bauxite, which is the first type of bauxite formed in the region, have the maximum value, while these values are at minimum levels in the bauxite group.

3.4. Distribution maps of geochemical results of the Sutlegen bauxite samples

The spatial distribution maps of the chemical analysis results of the samples were prepared using the GIS software of ArcMap 10.3.1 (Fig. 11a-d).

4. Discussion

4.1. Mineral genesis

High boehmite (56.34-46.04 wt%) and kaolinite contents (12.20-9.89 wt%) were detected in the XRD spectra of the bauxite samples.

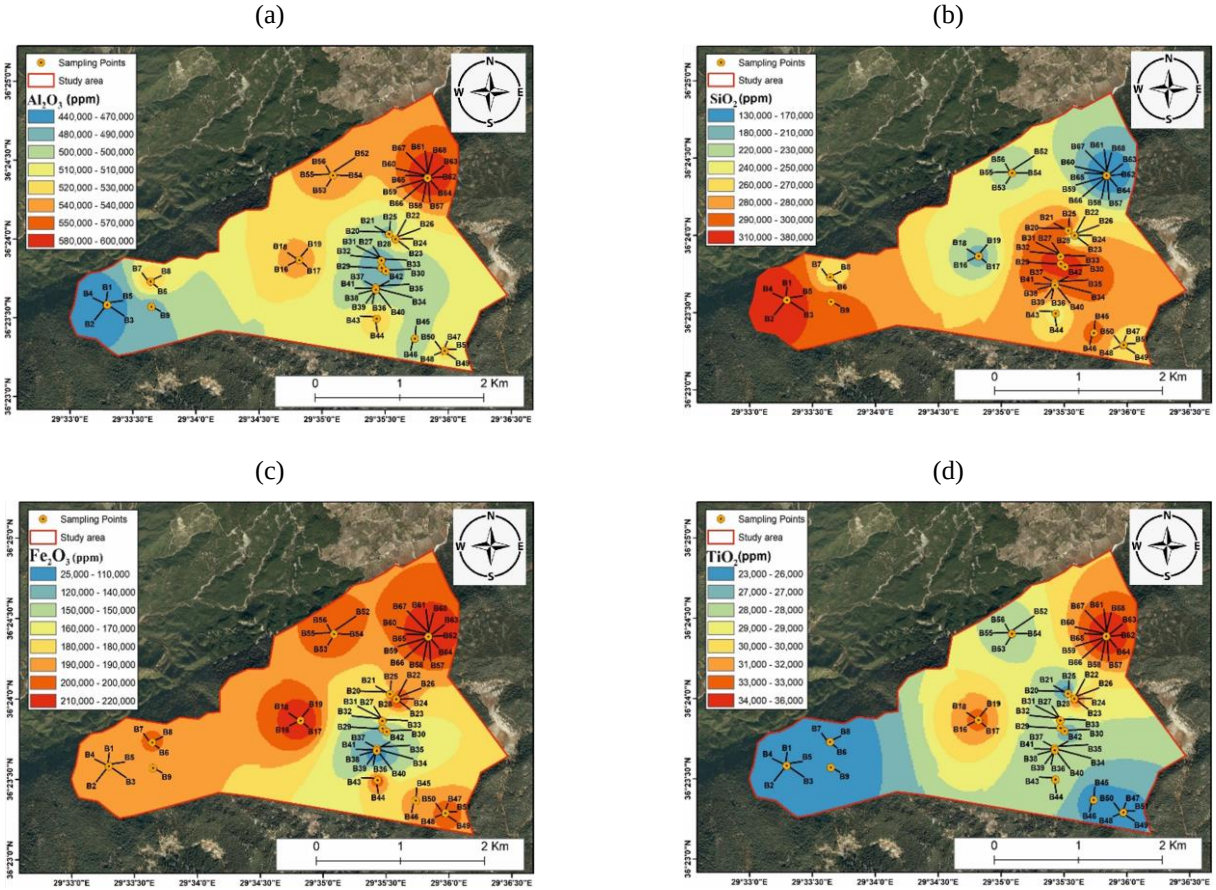

Figure 11. Regional distribution: (a) Al_2O_3; (b) SiO_2; (c) Fe_2O_3; (d) TiO_2

The dissolution of the silica and silicic acid disrupts the chemical content of kaolinite. Bauxitic kaolinite transforms into gibbsite, boehmite, or diaspore under the influence of depth and temperature [22], [64], [65]. In regions with high groundwater levels and regular precipitation conditions, gibbsite is more stable than boehmite mineral in bauxite ore. On the other hand, in regions with low groundwater levels and irregular precipitation conditions, boehmite mineral is more stable than gibbsite [66].

REEs are generally associated with Ti [6], [67], [68]. Alkali and alkaline earth elements are absorbed by clay minerals during the chemical decomposition process. The Cs, B, Rb elements are absorbed by clay minerals. The geochemical behavior of Hf, Nb, Ta, U, Th, Sc, Cr, and Ga depends on anatase and bauxitophile minerals. High Cr values are generally the sign of mafic and ultramafic origin [6].

4.2. Geochemical behaviors of major elements, trace elements, REEs

The immobile elements, major oxides, and rare earth elements proposed by [17] are used to reveal the parent rock properties of bauxite ores [17], [24], [44], [69]-[71]. The basic geochemical properties of bauxite ores are associated with reactions occurring in the parent rock [17], [72], [73]. The tendency of TiO_2 concentration to decrease from lateritic bauxite to bauxite samples may be associated with low pH conditions and the Ti-reducing bauxite sediments in the anatase mineral observed in the samples [74].

The ∑REE content values in similar studies carried out on the Taurus belt were found to range between 152.11-481.77 [9], [18], [21],[44]. The ∑REE contents of bauxite samples were found to be relatively lower (149.7 ppm). The REEs with the highest are as follows: Ce > Nd > Sc. Al_2O_3, SiO_2, and Fe_2O_3 have an insignificant role in absorbing the REE group elements [74]. In the light of this information, minerals transporting Al_2O_3, SiO_2, and Fe_2O_3 in bauxite ore. Minerals such as boehmite, kaolinite, hematite, gibbsite, goethite, and quartz are not thought to have an important role in absorbing REEs. The main chemical conditions of lateritic bauxite formation begin by the weathering of aluminosilicate minerals in the low pH environment and filtering of alkaline elements in the environment [75], [76].

The bauxite types in the Sutlegen region can be listed based on their Ce concentrations in descending order as follows: bauxite > kaolinitic bauxite > lateritic bauxite > ferritic bauxite. The Ce anomalies of bauxites developing in the paleokarstic environment are associated with their laterization and kaolinization processes. The Ce is expected to enrich during the bauxite formation [77]-[79].

4.3. The source of the parent rock of the Sutlegen bauxite ore and chemical weathering processes of bauxites

The bivariate diagram of Log Cr vs. Log Ni proposed by [80] provides important information on the parent source rocks of bauxite formation (Fig. 12a). According to mass change calculations of the Poci bauxites using the Log Cr vs. Log Ni diagram and TiO_2 values, the authors argued that these bauxites were mainly derived from felsic igneous rocks [3]. The Log Cr vs. R accumulation plot provides an understanding of the magmatic source, which plays a role in the formation of bauxites [81], [82] (Fig. 12b).

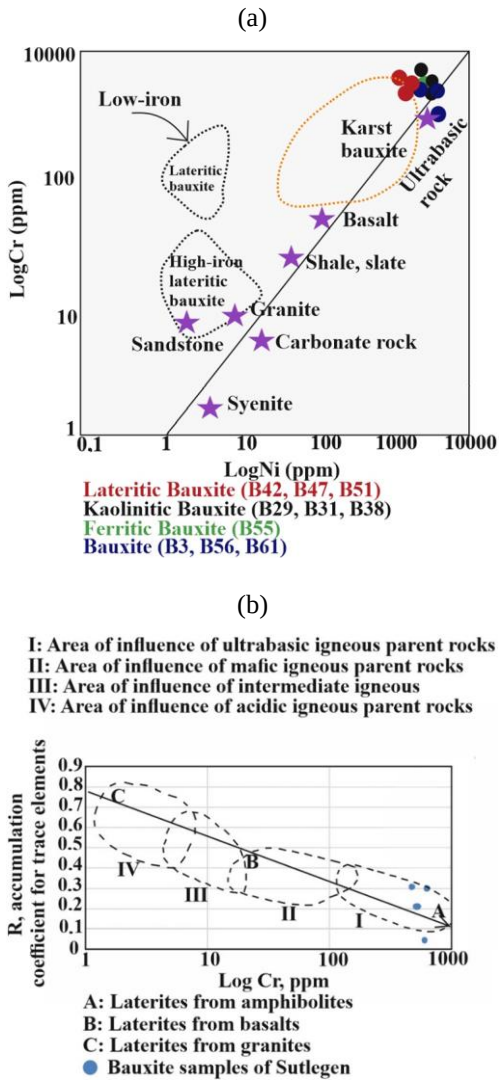

Figure 12. Charts determining the genesis of the Sutlegen bauxite: (a) plot of Ni versus Cr distribution diagram (after [80]); (b) log Cr versus accumulation coefficient values with the indication of areas of influence of various parent rocks [81], [82]

High Cr concentrations in bauxite samples indicate mafic or ultrabasic igneous rocks [3], [83], [84]. Karst-type bauxites have varying amounts of geochemical contents of Cu and Sb elements [3], [84], [85]. The Sutlegen bauxites have varying amounts of concentrations of Cu (606-51.4 ppm) and Sb (38.8-0 ppm).

Aluminous minerals can form bauxite ores when the environmental conditions related to weathering are met [86]. According to the previous results, lateritic bauxites have been affected by the physical and structural properties of the region's source rock [50], [64], [87]. However, this may not be the case for the karstic and sedimentary bauxites [26].

4.4. Formation mechanism of bauxites

Geochemical anomalies and the relationships of the bauxite samples taken from the region were examined. The first stage of bauxite formation in the Sutlegen region was considered to be the laterization reaction. During laterization, lateritic material, which was transported as a result of transgressive movements by superficial events (mechanical mobility), moved to Beydaglari formation, which consists of the Upper Cretaceous limestones. This movement occurs through Elmali formation, which covers the vast majority of the study area and consists of the Upper Lutetian-Lower Burdigalian sandstone, claystone, siltstone, and limestone [88]-[91]. As a result of these movements, the SiO_2 content in its chemical composition decreased, and it formed ferritic bauxite. Dendrogram analysis reveals that these two types of bauxites show the same geochemical properties. The lateritic zone, moving over the karstic limestones and other sedimentary units, filled the karstic cavities there. These karstic cavities underwent metamorphism, and the weathering processes began (Fig. 13).

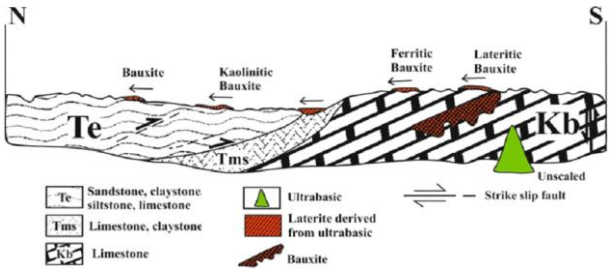

Figure 13. A geological model for the formation of the Sutlegen bauxite

5. Conclusion

According to the XRD and microscope images, the major minerals of bauxite samples were found to be boehmite, kaolinite, hematite, gibbsite, goethite, and anatase, while anorthite, quartz, and chamosite were the minor minerals. It was found that the mineralogical composition of lateritic bauxite was mostly characterized by hematite and goethite minerals. However, the samples were mostly characterized by boehmite and gibbsite minerals in the bauxite classification. Bauxite samples contain high contents of boehmite and kaolinite. Considering the tropical climate conditions in the bauxite formation environment, the boehmite mineral was formed due to the kaolinite/dehydration reactions' destruction. The formation of boehmite in the karstic cavities between the limestones of Upper Lutetian-Lower Burdigalian age and other sedimentary formations was associated with low-grade metamorphic tectonism. Also, the formation temperature of the samples in the Bauxite classification was considered to be between 140-200ºC. The presence of hematite observed in bauxite samples (15.17-7.72 wt%) played an active role in bauxite formation. It was considered that the kaolinite content tended to decrease with the increase of the hematite mineral in the formation environment. The XRD analyses revealed that Al-bearing minerals were boehmite, kaolinite, gibbsite, anorthite, and chamosite, while Fe-

bearing minerals were found to be hematite, goethite, and chamosite.

Al_2O_3-SiO_2-Fe_2O_3 diagrams were prepared using geochemical data. It was determined that bauxite ores have undergone moderate and strong laterization processes as a result of the deferruginization in the environment, and they were classified into the following four groups: lateritic bauxite, ferritic bauxite, kaolinitic bauxite, and bauxite.

In general, Al_2O_3, Fe_2O_3, TiO_2, and SiO_2 were found to be the major geochemical components of bauxite samples classified under four groups. The average Al_2O_3 and Fe_2O_3 values of the classified bauxite samples are as follows: lateritic (43.52 wt%, 33.02 wt%), ferritic (53.10 wt%, 19.70 wt%), kaolinitic (49.47 wt%, 8.00 wt%), and bauxite (50.81 wt%, 19.41 wt%), respectively. The Al_2O_3 increase in bauxites that undergo laterization processes is directly proportional to the formation mechanism. The lateritic material was transported and filled into the cavities and pores of karst-type limestones in the Sutlegen region. The bauxitic material formed karst-type bauxites by accumulating in these cavities. Karst-type bauxites have a higher SiO_2 concentration than other bauxite types formed in the region (25.43 wt%). Karst-type sediments and other carbonated rocks in the formation environment (alkaline conditions and pH balance) were considered to be the reason for this situation. The TiO_2 contents of the bauxite types are sorted in descending order as follows: lateritic bauxite (6.6 wt%), bauxite (3.7 wt%), kaolinitic bauxite (2.8 wt%), and ferritic bauxite (2.6 wt%). The mass change calculations prove that the lateritic bauxite, which is the first product of the bauxite formation mechanism in the Sutlegen region, contains the highest rates of TiO_2, and it depletes in the environment in laterization processes. The data obtained from immobile element analyses and their comparison with upper continental crust (UCC) data reveal the enrichment in the elements of V, Ni, Zn, Sr, Co, Y, Nb and depletion in the elements of Rb, Eu, Tb, Hf, K, and P.

The highest Ga content is observed in the samples classified as bauxite (61.15 ppm), and it is followed by ferritic bauxite samples (60 ppm), kaolinitic bauxite samples (59.27 ppm), and finally the lateritic bauxite samples (46.45 ppm). It was found that the bauxite formation started with laterization reactions, and the first bauxite formed was classified as the lateritic bauxite.

The bivariate plots of Log Cr vs. Log Ni prepared for Sutlegen bauxites revealed karstic and ultrabasic igneous rock sources. The Log Cr vs. R binary diagram proves that a magmatic source is associated with ultrabasic igneous rocks. The mass change calculations supported the idea that they had an ultrabasic igneous rock source. Considering the bauxite formation mechanism, it is seen that the behaviors of alkaline earth elements began to decrease at the beginning of the laterization process.

Lateritic bauxites in the region were found to have the highest WIP values. The WIP values are observed to decrease in the processes in which the formation phases continue (until the formation of the samples in the bauxite classification). Likewise, the R ratio also tended to decrease in lateritic bauxites followed by the bauxite samples classified as kaolinitic, ferritic, and bauxite.

Lateritic soil in the sample collection area is the first stage product of bauxite formation. When available conditions (tropical environment conditions) were provided in the formation environment, kaolinite mineral began to form in the soil. The geochemical data of the Sutlegen bauxites revealed that the source of laterization in the region was the ultrabasic igneous rocks. There is no direct evidence of ultrabasic igneous rock in the region. During the ongoing processes of laterization, lateritic formations, which were transported by sandstone, claystone, siltstone, and limestone as a result of transgressive movements by superficial events (mechanical mobility), accumulate in karstic cavities. Due to the effect of metamorphism, they formed karst-type bauxites that were classified as kaolinitic bauxite and bauxite.

Acknowledgements

The financial support for this research was provided by the Scientific Research Projects Coordination Unit (BAP, FKA-2019-4636) of Akdeniz University, Antalya/Turkey. The authors would like to thank the Scientific Research Projects Coordination Unit of Akdeniz University. This paper is a part of the M.Sc. thesis of Atakoglu Ozer O., the first author.

References

[1] Abedini, A., Khosravi, M., & Dill, H.G. (2020). Rare earth element geochemical characteristics of the late Permian Badamlu karst bauxite deposit, NW Iran. *Journal of African Earth Sciences*, (172), 103974. https://doi.org/10.1016/j.jafrearsci.2020.103974

[2] Borra, C.R., Blanpain, B., Pontikes, Y., Van, B.K., & Gerven. T. (2016). Recovery of rare earths and other valuable metals from bauxite residue (red mud): A review. *Journal of Sustainable Metallurgy*, *2*(4), 365-386. https://doi.org/10.1007/s40831-016-0068-2

[3] Yang, S., Huang, Y., Wang, Q., Deng, J., Liu, X., & Wang, J. (2019). Mineralogical and geochemical features of karst bauxites from Poci (western Henan. China). Implications for parental affinity and bauxitization. *Ore Geology Reviews*, (105), 295-309. https://doi.org/10.1016/j.oregeorev.2018.12.028

[4] Salamab-Ellahi, S., Taghipour. B., & Mongelli. G. (2019). Clayey bauxite from the Irano-Himalayan belt: Critical metals provenance and palaeoclimate in the Upper Cretaceous Semirom ore deposit. Zagros Mountain, Iran. *Journal of Asian Earth Sciences*, (172). 126-142. https://doi.org/10.1016/j.jseaes.2018.09.001

[5] Abedini, A., & Khosravi, M. (2020). Geochemical constraints on the Triassic-Jurassic Amir-Abad karst-type bauxite deposit, NW Iran. *Journal of Geochemical Exploration*, (211), 106489. https://doi.org/10.1016/j.gexplo.2020.106489

[6] Yang, S., Wang, Q., Deng, J., Wang, Y., Kang, W., Liu, X., & Li, Z. (2019). Genesis of karst bauxite-bearing sequences in Baofeng. Henan (China) and the distribution of critical metals. *Ore Geology Reviews*, (115), 103161. https://doi.org/10.1016/j.oregeorev.2019.103161

[7] Abedini, A., Khosravi, M., & Calagari, A.A. (2019). Geochemical characteristics of the Arbanos karst-type bauxite deposit. NW Iran: Implications for parental affinity and factors controlling the distribution of elements. *Journal of Geochemical Exploration*, (200), 249-265. https://doi.org/10.1016/j.gexplo.2018.09.004

[8] Authier-Martin, M., Forte, G., & Ostap, S. (2001). The mineralogy of bauxite for producing smelter-grade alumina. *JOM*, *53*(12), 36-40. https://doi.org/10.1007/s11837-001-0011-1

[9] Mongelli, G., Boni, M., Buccione, R., & Sinisi, R. (2014). Geochemistry of the Apulian karst bauxites (Southern Italy): Chemical fractionation and parental affinities. *Ore Geology Reviews*, (63), 9-21. https://doi.org/10.1016/j.oregeorev.2014.04.012

[10] Ahmadnejad, F., Zamanian, H., Taghipour, B., Zarasvandi, A., Buccione, R., & Ellah, S.S. (2017). Mineralogical and geochemical evolution of the Bidgol bauxite deposit. Zagros Mountain Belt. Iran: Implications for ore genesis rare earth elements fractionation and parental affinity. *Ore Geology Reviews*, (86), 755-783. https://doi.org/10.1016/j.oregeorev.2017.04.006

[11] Gamaletsos, P.N., Godelitsas. A., Kasama, T., Church, N.S., Douvalis, A.P., Göttlicher, J., Steininger, R., Boubnov, A., Pontikes, Y., Tzamos, E., Bakas, T., & Filippidis. A. (2017). Nano-mineralogy and geochemistry of high-grade diasporic karst-type bauxite from Parnassos-Ghiona mines, Greece. *Ore Geology Reviews*, (84), 228-244. https://doi.org/10.1016/j.oregeorev.2016.11.009

[12] Gamaletsos, P.N., Godelitsas, A., Filippidis, A., & Pontikes, Y. (2019). The rare earth elements potential of Greek bauxite active mines in the

light of a sustainable REE demand. *Journal of Sustainable Metallurgy*, *5*(1), 20-47. https://doi.org/10.1007/s40831-018-0192-2

[13] Khosravi, M., Abedini, A., Alipour, S., & Mongelli, G. (2017). The Darzi-Vali bauxite deposit. West-Azarbaidjan Province, Iran: Critical metals distribution and parental affinities. *Journal of African Earth Sciences*, (129), 960-972. https://doi.org/10.1016/j.jafrearsci.2017.02.024

[14] Radusinović, S., Jelenković, R., Pačevski, A., Simić, V., Božović, D., Holclajtner-Antunović, I., & Životić, D. (2017). Content and mode of occurrences of rare earth elements in the Zagrad karstic bauxite deposit (Nikšić area. Montenegro). *Ore Geology Reviews*, (80), 406-428. https://doi.org/10.1016/j.oregeorev.2016.05.026

[15] Ling, K.Y., Zhu, X.Q., Tang, H.S., Du, S.J., & Gu, J. (2018). Geology and geochemistry of the Xiaoshanba bauxite deposit. Central Guizhou Province, SW China: Implications for the behavior of trace and rare earth elements. *Journal of Geochemical Exploration*, (190), 170-186. https://doi.org/10.1016/j.gexplo.2018.03.007

[16] Abedini, A., Mongelli, G., Khosravi, M., & Sinisi, R. (2020). Geochemistry and secular trends in the middle-late Permian karst bauxite deposits, northwestern Iran. *Ore Geology Reviews*, (124), 103660. https://doi.org/10.1016/j.oregeorev.2020.103660

[17] MacLean, W.H., Bonavia, F.F., & Sanna, G. (1997). Argillite debris converted to bauxite during karst weathering: evidence from immobile element geochemistry at the Olmedo deposit, Sardinia. *Mineralium Deposita*, (32), 607-616. https://doi.org/10.1007/s001260050126

[18] Meshram, R.R., & Randive, K.R. (2011). Geochemical study of laterites of the Jamnagar district. Gujarat, India: Implications on parent rock mineralogy and tectonics. *Journal of Asian Earth Sciences*, (42), 1271-1287. https://doi.org/10.1016/j.jseaes.2011.07.014

[19] Yalcin, M.G., Karaman, M.E., & Alagoz, Z. (2012). Origin of the red soils in the Bolkardag region: Pınarkaya-Kayaonu case. (Karaman. Turkey). *International Multidisciplinary Scientific GeoConference: SGEM: Surveying Geology mining Ecology Management*, (4), 149. https://doi.org/10.5593/SGEM2012/S16.V4014

[20] Abedini, A., & Calagari, A.A. (2014). REE geochemical characteristics of titanium-rich bauxites: the Permian Kanigorgeh horizon, NW Iran. *Turkish Journal of Earth Sciences*, *23*(5), 513-532. https://doi.org/10.3906/yer-1404-11

[21] Yuste, A., Bauluz, B., & Mayayo, M.J. (2017). Origin and geochemical evolution from ferrallitized clays to karst bauxite: An example from the Lower Cretaceous of NE Spain. *Ore Geology Reviews*, (84), 67-79. https://doi.org/10.1016/j.oregeorev.2016.12.025

[22] Bárdossy, G. (1982). Karst bauxites bauxite deposits on carbonate rocks. *Developments in Economic Geology*, (14). https://doi.org/doi:10.1016/c2009-0-14505-1

[23] Bogatyrev, B.A., Zhukov, V.V., & Tsekhovsky. Y.G. (2009). Formation conditions and regularities of the distribution of large and superlarge bauxite deposits. *Lithology and Mineral Resources*, (44), 135-151. https://doi.org/10.1134/S0024490209020035

[24] Zamanian, H., Ahmadnejad, F., & Zarasvandi, A. (2015). Mineralogical and geochemical investigations of the Mombi bauxite deposit. Zagros Mountains, Iran. *Chemie der Erde – Geochemistry*, (76), 13-37. https://doi.org/10.1016/j.chemer.2015.10.001

[25] Nyamsari, D.G., & Yalcin, M.G. (2017). Statistical analysis and source rock of the Minim-Martap plateau bauxite, Cameroon. *Arabian Journal of Geosciences*, *10*(18), 415. https://doi.org/10.1007/s12517-017-3172-0

[26] Sidibe, M., & Yalcin, M.G. (2019). Petrography mineralogy geochemistry and genesis of the Balaya bauxite deposits in Kindia region, Maritime Guinea, West Africa. *Journal of African Earth Sciences*, (149), 348-366. https://doi.org/10.1016/j.jafrearsci.2018.08.017

[27] Oz, C., & Ozer, O. (2019). Application and Interpretation of spectroscopic methods in ceramic archaeometry: XRF, XRD. *The Journal of Ceramic Research*, (1), 136-153.

[28] Pinto, F.G., Junior, R.E., & Saint'Pierre, T.D. (2012). Sample preparation for determination of rare earth elements in geological samples by ICP-MS: A critical review. *Analytical Letters*, *45*(12), 1537-1556. https://doi.org/10.1080/00032719.2012.677778

[29] Senel, M. (1997). *1/250000 scale Geological Map of Turkey No. 2 to 6: Fethiye Pages*. Ankara, Turkey: MTA Publishing.

[30] Senel, M., Serdaroglu, M., Kengil, R., Unverdi, M., & Gozle, M.Z. (1981). Geology of Teke Taurus mountains southeast: *MTA Bulletin*, (95/96), 13-43.

[31] Senel, M. (1986). *1/250000 scale Geological Map of Turkey No. 2 to 6: Fethiye Pages*. Ankara, Turkey: MTA Publishing.

[32] Senel, M. (1989). *1/250000 scale Geological Map of Turkey No. 2 to 6: Fethiye Pages*. Ankara, Turkey: MTA Publishing.

[33] Senel, M. (1991). *1/250000 scale Geological Map of Turkey No. 2 to 6: Fethiye Pages*. Ankara, Turkey: MTA Publishing.

[34] Senel, M., (1994). *1/250000 scale Geological Map of Turkey No. 2 to 6: Fethiye Pages*. Ankara, Turkey: MTA Publishing.

[35] Senel, M. (1985). *1/25000 scale digital geological map, Fethiye P23 Plot of Turkey geological database, the geological survey department*. Ankara, Turkey: MTA Publishing.

[36] Baykal, F., & Onalan, M. (1979). Sile sedimentary (Sile Olistostromu) *Altinli Symposium* (pp. 15-25). Ankara, Turkey.

[37] Ocal, H. (1988). *1/25000 scale digital geological map, Fethiye P23 Plot of Turkey geological database, the geological survey department*. Ankara, Turkey: MTA Publishing.

[38] Gunay, Y., Bolukbasi, S., & Yoldemir, O. (1982). Stratigraphy and structure of the Beydaglari: *Abstracts of the 6th Petroleum Congress of Turkey* (pp. 91-101).

[39] Yalcin, M.G., Nyamsari, D.G., Atakoglu, O.O., & Yalcin, F. (2021). Chemical and statistical characterization of beach sand sediments: Implication for natural and anthropogenic origin and paleo-environment. *International Journal of Environmental Science and Technology*. https://doi.org/10.1007/s13762-021-03280-8

[40] Dangic, A. (1988). Kaolinization of bauxite: A study of the Vlasenica bauxite area Yugoslavia II. Alteration of oolites. *Clays and Clay Minerals*, (36), 439-447. https://doi.org/10.1346/CCMN.1985.0330606

[41] Meyer, F.M., Happel, U., Hausberg, J., & Wiechowski, A. (2002). The geometry and anatomy of the Los Pijiguaos bauxite deposit, Venezuela. *Ore Geology Reviews*, (20), 27-54. https://doi.org/10.1016/S0169-1368(02)00037-9

[42] Yalcin, M.G., & Ilhan, S. (2008). Major and trace element geochemistry of Terra Rossa soil in the Kucukkoras region. Karaman. Turkey. *Geochemistry International*, *46*(10), 1038. https://doi.org/10.1134/S001670290810008X

[43] Schellmann, W. (1982). Eine neue Lateritdefinition. *Geologisches Jahrbuch – Reihe D*, (58), 31-47.

[44] Gu, J., Huang, Z., Fan, H., Jin, Z., Yan, Z., & Zhang, J. (2013). Mineralogy: Geochemistry.and genesis of lateritic bauxite deposits in the Wuchuan-Zheng'an-Daozhenarea. Northern Guizhou Province, China. *Journal of Geochemical Exploration*, (130), 44-59. https://doi.org/10.22071/GSJ.2018.89035.1149

[45] Liu, X.F, Wang, Q., Feng, Y., Li, Z., & Cai, S. (2013). Genesis of the Guangou karstic bauxite deposit in western Henan, China. *Ore Geology Reviews*, (55), 162-175. https://doi.org/10.1016/j.oregeorev.2013.06.002

[46] Schulte, R.F., & Foley, N.K. (2013). *Compilation of gallium resource data for bauxite deposits (No. 2013-1272)*. New York, United State: US Geological Survey.

[47] Ozer, O., & Yalcin, M.G. (2020). Correlation of chemical contents of Sutlegen (Antalya) bauxites and regression analysis. *AIP Conference Proceedings*, (2293), 180008. https://doi.org/10.1063/5.0026731

[48] Aleva, G.J.J. (1994). *Laterites: Concepts geology morphology and chemistry*. International Soil Reference and Information Centre (ISRIC).

[49] Sun, S.S., & McDonough, W.F. (1989). Chemical and isotopic systematics of oceanic basalts: Implications for mantle composition and processes. *Geological Society*, (42), 313-345.

[50] Bárdossy, G., & Aleva. G. J.J. (1990). *Lateritic bauxites*. London, United Kingdom: Elsevier Science Ltd.

[51] Boulangé, B., & Carvalho, A. (1997). The bauxite of Porto Trombetas Brazilian Bauxites. *USP/FAPESP/ORSTOM*, 55-73.

[52] Beauvais, A., & Colin. F. (1993). Formation and transformation processes of iron duricrust systems in tropical humid environment. *Chemical Geology*, *106*(1-2), 77-101. https://doi.org/10.1016/0009-2541(93)90167-H

[53] Tardy, Y. (1997). *Petrology of laterites and tropical soils*. London, United Kingdom: Balkema, 408 p.

[54] Bárdossy, G., & Combes, P.J. (1999). Karst bauxites: interfingering of deposition and palaeoweathering. In: Thiry, M., Simon-Coincon, R. (Eds.). Paleoweathering. Paleo surfaces and related continental deposits. *International Association of Sedimentologists*, (27), 189-206.

[55] Nyamsari, D.G., Yalcin, F., Mboh, M.T., Alfred, F.G., & Yalcin, M.G. (2019). Natural radioactive risk assessment in top soil and possible health effect in Minim and Martap villages. Cameroon: Using radioactive risk index and statistical analysis. *Kerntechnik*, *84*(2), 115-122. https://doi.org/10.3139/124.110927

[56] Taylor, S.R., & McLennan, S.M. (1981). The composition and evolution of the continental crust: rare earth element evidence from sedimentary rocks. *Philosophical Transactions of the Royal Society of London. Series A. Mathematical and Physical Sciences*, *301*(1461), 381-399. https://doi.org/10.1098/rsta.1981.0119

[57] Taylor, S.R., & McLennan, S.M. (1995). The geochemical evolution of the continental crust. *Reviews of Geophysics*, *33*(2), 241-265. https://doi.org/10.1029/95RG00262

[58] Ozer Atakoglu, O., Yalcin, M.G., & Ozmen, S.F. (2021). Determination of radiological hazard parameters and radioactivity concentrations in bauxite samples: The case of the Sutlegen Mine Region (Antalya,

Turkey). *Journal of Radioanalytical and Nuclear Chemistry*, *329*(2), 701-715. https://doi.org/10.1007/s10967-021-07826-5
[59] Parker, A. (1970). An index of weathering for silicate rocks. *Geological Magazine*, (107), 501-504. https://doi.org/10.1017/S0016756800058581
[60] Fedo, C.M., Nesbitt, H.W., & Young, G.M. (1995). Unravelling the effects of potassium metasomatism in sedimentary rocks and paleosols with implications for paleoweathering conditions and provenance. *Geology*, (23), 921-924. https://doi.org/10.1130/0091-7613(1995)023<0921:UTEOPM>2.3.CO;2
[61] Nesbitt, H.W., & Young, G.M. (1982). Early Proterozoic climates and plate motions inferred from major element chemistry of lutite. *Nature*, (299), 715-717. https://doi.org/10.1038/299715a0
[62] Price, J.R., & Velbel, M.A. (2003). Chemical weathering indices applied to weathering profiles developed on heterogeneous felsic metamorphic parent rocks. *Chemical Geology*, (202), 397-416. https://doi.org/10.1016/j.chemgeo.2002.11.001
[63] Ruxton, B.P. (1968). Measures of the degree of chemical weathering of rocks. *Journal of Geology*, (76), 518-527. https://doi.org/10.1086/627357
[64] Yalcin, M.G., & Ilhan, S. (2013). Major and trace element geochemistry of bauxites of Ayranci, Karaman, Central Bolkardag, Turkey. *Asian Journal of Chemistry*, *25*(5), 2893-2904. http://dx.doi.org/10.14233/ajchem.2013.14275
[65] Denigres, F., Rocha, G.D.A., Montes, C.R., & Vieira-Coelho, A.C. (2016). Synthesis and characterization of boehmites obtained from gibbsite in presence of different environments. *Materials Research*, *19*(3), 659-668. https://doi.org/10.1590/1980-5373-MR-2016-0019
[66] Tardy, Y., Valeton, I., & Melfi, A. (1988). Climats et paleoclimats tropicaux piriatlantiques. Rôle des facteurs climatiques et thermodynamiques: Température et activité de l'eau, sur la répartition et la composition minéralogique des bauxites et des cuirasses ferrugineuses, au Brésil et en Afrique. Comptes Rendus. *Académie des Sciences*, *306*(11), 289-295.
[67] Krishnamurthy, N., & Gupta, C.K. (2015). *Extractive metallurgy of rare Earths*. Florida, United States: CRC Press.
[68] Li, G., Ye, Q., Deng, B., Luo, J., Rao, M., Peng, Z., & Jiang, T. (2018). Extraction of scandium from scandium-rich material derived from bauxite ore residues. *Hydrometallurgy*, (176), 62-68. https://doi.org/10.1016/j.hydromet.2018.01.007
[69] Maclean, W.H. (1990). Mass change calculations in altered rock series. *Mineralium Deposita*, (25), 44-49. https://doi.org/10.1007/BF03326382
[70] Calagari, A.A., & Abedini, A. (2007). Geochemical investigations on Permo-Triassic bauxite horizon at Kanisheeteh east of Bukan, West-Azarbaidjan, Iran. *Journal of Geochemical Exploration*, *94*(1-3), 1-18. https://doi.org/10.1016/j.gexplo.2007.04.003
[71] Ozer, O., & Yalcin, M.G. (2019). Modeling of elemental distribution of Kas (Antalya) bauxite deposit II. *International Conference of Numerical Analysis and Applied Mathematics*. Rhodes. Greece.
[72] Hill, I.G., Worden, R.H., & Meighan, I.G. (2000). Geochemical evolution of a palaeolaterite: The interbasaltic formation, Northern Ireland. *Chemical Geology*, *166*(1), 65-84. https://doi.org/10.1016/S0009-2541(99)00179-5
[73] Patino, L.C., Velbel, M.A., Price, J.R., & Wade, J.A. (2003). Trace element mobility during spheroidal weathering of basalts and andesites in Hawaii and Guatemala. *Chemical Geology*, *202*(3-4), 343-364. https://doi.org/10.1016/j.chemgeo.2003.01.002
[74] Ozlu, N. (1984). New facts on diaspore genesis in the Aksek-Seydisehir bauxite deposits (Western Taurus, Turkey). *Travaux du Comité International Pour L'étude des Bauxites de L'alumine et de L'aluminium*, (14), 53-62.
[75] Bland, W., & Rolls, D. (1998). *Weathering: An introduction to scientific principles*. London, United Kingdom: Arnold.
[76] Raiswell, R.W., Brimblecombe, P., Dent, D.L., & Liss, P.S. (1980). *Environmental chemistry: The earth air-water factory*. New Jersy, United States: John Wiley & Sons.
[77] Braun, J.J., Pagel, M., Muller, J.P., Bilong, P., Michard, A., & Guillet, B. (1990). Ceriumanomalies in lateritic profiles. Geochim. *Cosmochimia Acta*, (54), 781-795. https://doi.org/10.1016/0016-7037(90)90373-S
[78] Nyakairu, G.W., Koeberl, C., & Kurzweil, H. (2001). The Buwambo kaolin deposit in central Uganda: Mineralogical and chemical composition. *Geochemical Journal*, *35*(4), 245-256. https://doi.org/10.2343/geochemj.35.245
[79] Compton, J.S., White, R.A., & Smith, M. (2003). Rare earth element behavior in soils and salt pan sediments of a semi-arid granitic terrain in the Western Cape, South Africa. *Chemical Geology*, *201*(3-4), 239-255. https://doi.org/10.1016/S0009-2541(03)00239-0
[80] Schroll, E., & Sauer, D. (1968). Beitrag zur Geochemie von Titan, Chrom, Nickel, Cobalt, Vanadium und Molyb din in bauxitischen Gesteinen und das Problem der stofflichen Herkunft des Aluminiums. *Travaux du ICSOBA*, (5), 83-96.
[81] Ozlu, N. (1983). Trace element contents of karst bauxites and their parent rocks in the Mediterranean belt. *Mineralium Deposita*, (18), 469-476.
[82] Nyamsari, D.G., Yalcin, M.G., & Wolfson, I. (2020). Alteration, chemical processes, and parent rocks of Haléo-Danielle Plateau bauxite, Adamawa-Cameroon. *Lithology and Mineral Resources*, (55), 231-243. https://doi.org/10.1134/S0024490220030049
[83] Mongelli, G., Boni, M., Oggiano, G., Mameli, P., Sinisi, R., Buccione, R., & Mondillo, N. (2017). Critical metals distribution in Tethyan karst bauxite: The cretaceous Italian ores. *Ore Geology Reviews*, (86), 526-536. https://doi.org/10.1016/j.oregeorev.2017.03.017
[84] Putzolu, F., Piccolo Papa, A., Mondillo, N., Boni, M., Balassone, G., & Mormone, A. (2018). Geochemical characterization of bauxite deposits from the Abruzzi mining district (Italy). *Minerals*, (8), 298. https://doi.org/10.3390/min8070298
[85] Salamab-Ellahi, S., Taghipour, B., & Nejadhadad, M. (2017). The role of organic matter in the formation of high-grade Al deposits of the Dopolan karst type bauxite, Iran: Mineralogy, geochemistry, and sulfur isotope data. *Minerals*, (7), 97. https://doi.org/10. 3390/min7060097
[86] Patterson, S.H., Kurtz, H.F., Olson, J.C., & Neeley, C.L. (1986). World bauxite resources. *U.S. Geological Survey. Professional Paper*. 1076B. Washington, United States: U.S. Government Printing Office.
[87] Mondillo, N., Balassone, G., Boni, M., & Rollinson, G.G. (2011). Karst bauxites in the Campania Apennines (southern Italy): A new approach. *Periodico di Mineralogia*, *80*(3), 407-432. https://doi.org/10.2451/2011PM0028
[88] Ince, Z., Atakoglu, O.O., & Yalcin, M.G. (2021). Multivariate and spatial statistical analysis of geochemical data of dolomite: The case of industrial raw materials' differentiation. *Montes Taurus Journal of Pure and Applied Mathematics*, *3*(2), 8-28.
[89] Yalcin, M.G., Nyamsari, D.G., Paksu, E., & Yalcin, F. (2016). Statistical assessment of rare earth elements of bauxite deposits of Minim-Martap Plateau, Cameroon. *International Multidisciplinary Scientific GeoConference: Surveying Geology Mining Ecology Management*, (2), 819-825. https://doi.org/10.5593/sgem2016/b12/s03.105
[90] Ozer, O., Yalcin, F., Tarinc, O.K., & Yalcin, M.G. (2020). Investigation of suitability of marbles to standards with inequality expressions and statistical approach using some physical and mechanical properties. *Journal of Inequalities and Applications*, *2020*(1), 1-15. https://doi.org/10.1186/s13660-020-02360-6
[91] Kursun, G.B., & Yalcin, M.G. (2020). Origin of barite deposits in dolomite-limestone units, Gazipasa, Eastern of Antalya: Geology, geochemistry, statistics, sulfur isotope composition. *Mining of Mineral Deposits*, *14*(1), 62-71. https://doi.org/10.33271/mining14.01.062

Геохімічні особливості родовища бокситів у Сутлегені, Південно-Західна Анталія

О.О. Атакоглу, М.Г. Ялчин

Мета. Визначити геологічні та геохімічні характеристики бокситів у Сутлегені (Анталія, Туреччина) і встановити значення хімічних елементів в їх утворенні.

Методика. Був використаний аналіз мінеральної фази методом рентгенівської дифракції, рентгенофлуоресцентний елементний аналіз, мас-спектрометрія з індуктивно-зв'язаною плазмою, петрографічний і мінералогічний аналіз, різноманітні статистичні методи.

Результати. Визначено основний елементний склад руди: Al_2O_3 (60-35.2% ваг.), SiO_2 (39.5-0.2% ваг.), Fe_2O_3 (48.4-19.5% ваг.), TiO_2 (36.9-16% ваг.) і P_2O_5 (0.5-0.1% ваг.). Визначено, що Сутлеген, що з'явився в результаті епірогенетичних процесів і підйому земної кори, багатий нерітичними карбонатами. Встановлено, що бокситові руди піддавалися помірній та сильній латеритизації через знезалізнення місцевості. Руди були класифіковані й розділені на 4 групи: латеритові, феритові, каолінітові та бокситові. Збільшення кількості алюмосилікатних мінералів, які утворилися одночасно з бокситами, виявилося прямо пропорційним процесам латеритизації. Доведено, що латеритний матеріал, який утворився спочатку, заповнював пори і карстові порожнини вапняку та інших осадових утворень завдяки явищу поверхневого перенесення. З двохваріантних діаграм Log Cr і Log Ni слідує, що боксит, що утворився в даному регіоні, має ультраосновного походження.

Наукова новизна. Вперше для Сутлегенського родовища виявлено його геологічні та геохімічні особливості й описаний механізм його утворення. У науковій літературі відсутні дослідження щодо мінералізації бокситів Сутлегенського родовища, яке розробляється протягом багатьох років.

Практична значимість. Геохімічні характеристики бокситів дозволяють стверджувати, що джерелом процесу латеритизації в регіоні були ультраосновні магматичні породи. Латеритний матеріал завдяки поверхневому переносу накопичувався на пісковику, аргіліті, алевроліті, вапняку і в карстових порожнинах. Процеси метаморфізму згодом призвели до утворення карстового бокситу (каолінітового та бокситового) різних типів.

Ключові слова: *карстовий боксит, латеритний боксит, геохімія, мінералогія, петрографія, багатоваріантна статистика*

Геохимические особенности месторождения бокситов в Сутлегене, Юго-Западная Анталия

О.О. Атакоглу, М.Г. Ялчин

Цель. Определить геологические и геохимические характеристики бокситов в Сутлегене (Анталия, Турция) и установить значение химических элементов в их образовании.

Методика. Был использован анализ минеральной фазы методом рентгеновской дифракции, рентгенофлуоресцентный элементный анализ, масс-спектрометрия с индуктивно-связанной плазмой, петрографический и минералогический анализы, многовариантные статистические методы.

Результаты. Определен основной элементный состав руды: Al_2O_3 (60-35.2% вес.), SiO_2 (39.5-0.2% вес.), Fe_2O_3 (48.4-19.5% вес.), TiO_2 (36.9-16% вес.) и P_2O_5 (0.5-0.1% вес.). Определено, что Сутлеген, появившийся в результате эпирогенетических процессов и подъема земной коры, изобилует неритическими карбонатами. Установлено, что бокситовые руды подвергались умеренной и сильной латеритизации из-за обезжелезивания местности. Руды были классифицированы и разделены на 4 группы: латеритовые, ферритовые, каолинитовые и бокситовые. Увеличение количества алюмосиликатных минералов, которые образовались одновременно с бокситами, оказалось прямо пропорциональным процессам латеритизации. Доказано, что латеритный материал, который образовался вначале, заполнял поры и карстовые полости известняка и других осадочных образований благодаря явлению поверхностного переноса. Из двухвариантных диаграмм Log Cr и Log Ni следует, что боксит, образовавшийся в данном регионе, имеет ультраосновное происхождение.

Научная новизна. Впервые для Сутлегенского месторождения выявлены его геологические и геохимические особенности и описан механизм его образования. В научной литературе отсутствуют исследования по минерализации бокситов Сутлегенского месторождения, которое разрабатывается в течение многих лет.

Практическая значимость. Геохимические характеристики бокситов позволяют утверждать, что источником процесса латеритизации в регионе были ультраосновные магматические породы. Латеритный материал благодаря поверхностному переносу накапливался на песчанике, аргиллите, алевролите, известняке и в карстовых полостях. Процессы метаморфизма впоследствии привели к образованию карстового боксита (каолинитового и бокситового) различных типов.

Ключевые слова: *карстовый боксит, латеритный боксит, геохимия, минералогия, петрография, многовариантная статистика*